A direct ab initio molecular dynamics study of the finite temperature effects on the hyperfine coupling constant of methyl radical–water complexes

ARTICLE *in* JOURNAL OF MOLECULAR STRUCTURE THEOCHEM · OCTOBER 2002

Impact Factor: 1.37 · DOI: 10.1016/S0166-1280(02)00338-X

3 AUTHORS, INCLUDING:

Hiroto Tachikawa
Hokkaido University
284 PUBLICATIONS **2,976** CITATIONS

ELSEVIER

Journal of Molecular Structure (Theochem) 594 (2002) 61–69

THEO CHEM

www.elsevier.com/locate/theochem

A direct ab initio molecular dynamics study of the finite temperature effects on the hyperfine coupling constant of methyl radical–water complexes

Manabu Igarashi[a], Teruo Ishibashi[a], Hiroto Tachikawa[b,*]

[a]*Department of Biochemistry, Graduate School of Medicine, Hokkaido University, Sapporo 060-8638, Japan*
[b]*Division of Molecular Chemistry, Graduate School of Engineering, Hokkaido University, Kita-ku, Sapporo 060-8628, Japan*

Received 4 March 2002; revised 21 May 2002; accepted 6 June 2002

Abstract

Temperature and solvation effects on the hyperfine coupling constants (HFCCs) of methyl radical have been investigated by means of direct ab initio molecular dynamics (MD) method. The complexes composed of methyl radical and H_2O molecules, $CH_3(H_2O)_n$ ($n = 0–2$), were chosen as models of the solvation systems. The geometry optimizations of $CH_3(H_2O)$ showed that the hydrogen of H_2O molecule orients toward the carbon of CH_3, and it is weakly bound to the carbon atom of CH_3. The binding energies for $n = 1$ and $n = 2$ were calculated to be 1.50 and 2.82 kcal/mol at the MP2/6-311++G(d,p) level, respectively. The direct ab initio MD calculations indicated large temperature dependence of HFCCs: hydrogen-HFCC of CH_3 decreases with increasing temperature. This large change is due to the fact that the structure of the complex is flexible and is significantly varied by thermal activation. Mechanism of the temperature dependence of HFCCs was discussed on the basis of theoretical results.

Keywords: Molecular dynamics; Potential energy; Trajectory calculations

1. Introduction

Methyl radical (CH_3) is a simple prototype for a wide class of organic radicals which play an important role as an intermediate in biochemistry and also in radiation chemistry [1–3]. Consequently, the structure, electronic states, and reactivity of methyl radical have been extensively studied from both experimental and theoretical points of view [4–7].

The electron spin resonance (ESR) spectroscopy is one of the powerful tools for determining the electronic states of organic radicals [3,8–10]. The ESR experiments of CH_3 in several matrices revealed that methyl radical can form easily weakly bonded complexes with several molecules at low temperature. Misochko et al. [11] detected an intermediate in the hydrogen abstraction reaction by F atom from CH_4 molecule in Ar matrix,

$$F + CH_4 \text{ (reactant)}$$

$$\rightarrow F\cdots H\cdots CH_3 \text{ (Transition state, TS)}$$

$$TS \rightarrow HF\cdots CH_3 \text{ (intermediate)}$$

by means of ESR measurement. They observed the hyperfine coupling constant (HFCC) of the intermediate complex and indicated that the intermediate is

* Corresponding author. Fax: +81-11706-7897.
E-mail address: hiroto@eng.hokudai.ac.jp (H. Tachikawa).

0166-1280/02/$ - see front matter
PII: S0166-1280(02)00338-X

composed of the CH_3 radical and the HF molecule, i.e. the complex $H_3C\cdots HF$. Also, they showed that an unpaired electron in the complex is mainly localized on methyl carbon, but slightly diffused to the hydrogen of HF molecule. This result suggests that the HF molecule is weakly bound to the CH_3 radical by the hydrogen bond in which the hydrogen of HF coordinates toward the methyl carbon.

In a previous study, we applied direct ab initio molecular dynamics (MD) calculation to the $CH_3\cdots HF$ complex in order to predict temperature effect on HFCCs of the complex [12]. The calculations showed that HFCCs of the complex are strongly affected by thermal activation: i.e. hydrogen-HFCC increased gradually with increasing temperature. Also, it was found that the hydrogen of HF is very flexible around CH_3 radical. Recently, we have investigated thermal effects on HFCC of CH_3 by means of direct ab initio dynamics trajectory method [13]. The HFCC of the hydrogen of CH_3 increased with increasing temperature, which is in good agreement with ESR experiments [14].

The experimental works on the HFCC of the other weakly bonded complexes have been made by several workers [15]. Infrared spectroscopy has been applied to detect the complex and to elucidate the interaction between CH_3 and molecules. From the theoretical points of view, the static properties of weakly bonded complexes such as $H_3C\cdots CH_4$, $H_3C\cdots Ar$, and $H_3C\cdots HCl$ have been investigated by mainly ab initio MO calculations [16,17]. However, information on the dynamics feature of the weakly bonded complex of CH_3 (i.e. finite temperature effect) is scarcely known.

In the present paper, we investigated the methyl radical–water complexes $CH_3(H_2O)_n$ $(n = 1–2)$ using direct ab initio MD calculation in order to predict temperature effects on HFCCs of the complexes. This study would correspond to the determination of solvation effect on the HFCC of CH_3 radical. Therefore, it is important to study the complexes.

2. Methods of the calculations

2.1. Ab initio MO calculation

The complexes composed of methyl radical and water molecules were chosen as models of methyl radical–water system. Geometries for the complexes were fully optimized at the UHF/6-31G(d), and UMP2/6-311++G(d,p) levels of theory [18]. Since the HFCCs of the radicals have been known to be strongly affected by electron correlation and the choice of basis sets, we carefully checked the effects of the basis sets and electron correlation on the calculated. By considering these effects, HFCCs of the complexes were calculated by means of the MP2/6-311++G(d,p) level at each selected point of the trajectory calculation. In all calculations, the expected values of $\langle S^2\rangle$ without spin annihilation were smaller than 0.7605.

2.2. Direct ab initio molecular dynamics calculation

In the present system, degrees of freedom are $3N - 6 = 15$ $(N = 1)$ and 24 $(N = 2)$. Hence, we applied the direct ab initio MD calculation with all degrees of freedom for the methyl radical–water systems. Detail of direct ab initio MD method is described in Refs. [19–24].

In the direct ab initio MD calculation, we used 6-31G(d) basis set for the complexes throughout. Initial structures of the complex were chosen as the optimized one. The trajectories are calculated at several temperatures defined by

$$T = \frac{1}{3Nk}\left\langle \sum_{i=1}^{N} m_i v_i^2 \right\rangle$$

where N is number of atoms, v_i and m_i are velocity and mass of ith atom, and k is Boltzmann constant. The potential energy (total energy) and energy gradient were calculated at each time step. We assumed that each atom moves as a classical particle on the 6-31G(d) multi-dimensional potential energy surface. The equations of motion for n atoms in a complex are given by

$$\frac{dQ_j}{dt} = \frac{\partial H}{\partial P_j}$$

$$\frac{dP_j}{dt} = -\frac{\partial H}{\partial Q_j} = -\frac{\partial U}{\partial Q_j}$$

where $j = 1 - 3N$, H is classical Hamiltonian, Q_j is Cartesian coordinate of jth mode and P_j is conjugated momentum. These equations were numerically solved

by the Runge–Kutta method. No symmetry restriction was applied to the calculation of the energy gradients. The time step size was chosen by 0.50 fs, and a total of 2000 step was calculated for each simulation. A total of 20 snapshots of the trajectory were sampled at every 50 fs intervals and then the HFCC was averaged for each temperature. The drift of the total energy was confirmed to be less than 0.1% throughout at all steps in the trajectory. The momenta of the center of mass and the angular momenta around the center of mass were also confirmed to retain at the initial value of zero.

3. Results

3.1. Ab initio MO calculations

3.1.1. Structure of $CH_3(H_2O)_n$ complex

The structures of the $CH_3(H_2O)_n$ ($n = 0–2$) complexes were fully optimized at the several levels of theory. The optimized structures of the complexes obtained by MP2/6-311++G(d,p) level were schematically illustrated in Fig. 1. The optimized parameters obtained at the HF/6-31G(d) and MP2/6-311++G(d,p) levels are listed in Table 1. Both calculations gave the similar results on the structures of the complexes. The MP2 calculations of $CH_3(H_2O)$ indicated that the intermolecular distance between CH_3 and H_2O (R_{CO}) is calculated to be 3.4591 Å for the carbon–hydrogen distance. The proton of the H_2O molecule coordinates toward the methyl carbon in the most stable form. The C–H distance of CH_3 in the complex was calculated to be 1.0804 Å which is significantly close to that of the free CH_3 molecule (1.0800 Å). For $CH_3(H_2O)_2$, as well as $CH_3(H_2O)$, one of the water molecules orients toward the carbon of CH_3. The intermolecular distance (R_{CO}) was calculated to be 3.3638 Å, which is slightly shorter than that of $CH_3(H_2O)$ ($R_{CO} = 3.4591$ Å). The second water binds to the first water molecule by hydrogen bond and also binds to the methyl radical. Namely, water dimer orients to the methyl radical. It should be noted that the bending angles of CH_3 moiety in $CH_3(H_2O)_n$ ($n = 1–2$) were calculated to be $\langle\phi\rangle = 119.8°$ ($n = 1$) and 119.5° ($n = 2$), suggesting that CH_3 moiety has non-planar structure in the complexes.

The HFCCs were calculated at the MP2/6-311++G(d,p) level using the MP2/6-311++G(d,p) optimized structures. The results are summarized in Table 2. For the methyl radical without water, hydrogen-HFCC (H-HFCC) was calculated to be −27.17 G at the MP2/6-311++G(d,p)//MP2/6-311++G(d,p) level. H-HFCC largely decreased by the interaction with water molecules: −26.28 G for $n = 1$ and −25.69 G for $n = 2$. Also, it should be noted that the numerical values of MP2/6-311++G(d,p)//HF/6-31G(d) calculations were in reasonable agreement with those of MP2/6-311++G(d,p)//MP2/6-311++G(d,p) level. Hence, we calculated HFCC of $CH_3(H_2O)_n$ including the dynamical effects at the MP2/6-311++G(d,p)//HF/6-31G(d) level of theory throughout.

For CH_3, potential energy curves (PECs) were calculated along the A″ bending mode of CH_3 (Fig. 2(A)), together with H- and C-HFCCs of CH_3 (Fig. 2(B) and (C), respectively). PECs were calculated at the HF/6-31G(d), MP2/6-311++G(d,p) and QCISD/6-311++G(3df,3pd) levels of theory, and HFCCs were calculated at MP2/6-311++G(d,p) level. The potential energies were monotonously increased as a function of Φ. Also, both H- and C-HFCCs of CH_3 increased with increasing angle Φ. PEC calculated at the HF/6-31G(d) level was in good agreement with those of MP2 and QCISD calculations, meaning that HF/6-31G(d) calculation would give a reasonable feature for bending motion of CH_3.

For $CH_3(H_2O)$ complex, potential energy curves (PECs) calculated at HF/6-31(d) and MP2/6-311++G(d,p) levels are plotted in Fig. 3 as a function of bending angle θ. PEC for CH_3 is also plotted by dashed line in Fig. 3(A) for comparison. The minimum of PEC of CH_3 was located at $\theta = 90°$, whereas that of CH_3 in $CH_3(H_2O)$ was 93° (MP2). This means that the methyl radical has a bent form in $CH_3(H_2O)$ (bending angle $\langle\phi\rangle$ was calculated to be 119.6 Table 1). This structural deformation causes a change of HFCCs of CH_3: H-HFCC of CH_3 in $CH_3(H_2O)$ is calculated to be −26.28 G which is larger than that of CH_3 (−27.12 G) (Table 2). The value of C-HFCC was also changed by the complex formation. This difference of HFCCs is enough to detect using usual EPR measurement.

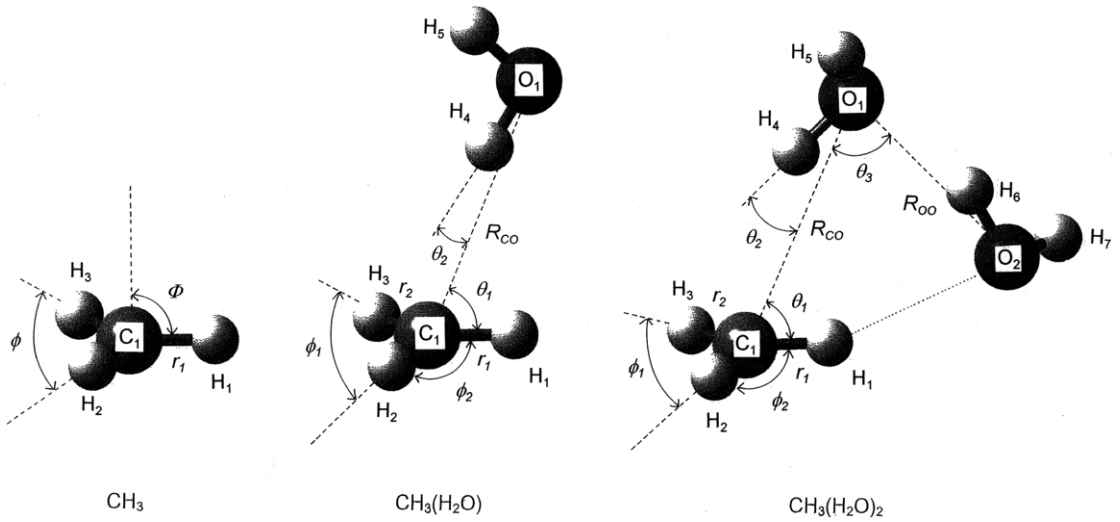

Fig. 1. Optimized structures of CH_3, $CH_3(H_2O)$ and $CH_3(H_2O)_2$ calculated at the MP2/6-311++G(d,p) level, and geometrical parameters.

3.1.2. Harmonic vibrational frequencies of the complexes $CH_3(H_2O)_n$ ($n = 0$, 1 and 2)

Table 3 shows the harmonic vibrational frequencies of $CH_3(H_2O)_n$ (n = 0, 1 and 2) calculated at the HF/6-31G(d) and MP2/6-311++G(d,p) levels of theory. For CH_3, the vibrational mode with a highest frequency (3360 cm^{-1}) corresponds to C–H stretching mode of CH_3. The lowest frequency calculated to be 463 cm^{-1} is the umbrella bending mode of CH_3 (A'' mode). By interacting with H_2O, the frequency of the A'' bending mode of CH_3 was increased (463 vs 547 cm^{-1}). This is due to the fact that the bending motion of CH_3 is restricted by interacting with H_2O: namely, hydrogen bond is formed between CH_3 and H_2O.

Table 1
Optimized geometrical parameters of $CH_3(H_2O)_n$ ($n = 0$, 1, 2). Bond lengths and angles are in Å and degrees, respectively

		HF/6-31G(d)	MP2/6-311++G(d,p)
CH_3	r_1	1.0726	1.0800
(D_{3h})	ϕ	120.0	120.0
$CH_3(H_2O)$	r_1	1.0734	1.0804
(C_s)	r_2	1.0734	1.0801
	R_{CO}	3.6245	3.4591
	ϕ_1	119.5	119.8
	ϕ_2	119.6	119.8
	θ_1	89.4	78.3
	θ_2	3.7	9.5
	$\langle\phi\rangle$[a]	119.6	119.8
$CH_3(H_2O)_2$	r_1	1.0738	1.0821
(C_1)	r_2	1.0740	1.0811
	R_{CO}	3.4886	3.3638
	R_{OO}	2.9409	2.8568
	ϕ_1	118.9	119.1
	ϕ_2	119.8	120.0
	θ_1	66.5	65.7
	θ_2	23.1	23.8
	θ_3	68.8	68.1
	$\langle\phi\rangle$[a]	119.4	119.5

[a] Average of value of ϕ_1 and ϕ_2.

The harmonic vibrational frequencies were also calculated at the HF/6-31G(d) level, and those are given in parenthesis in Table 3. As clearly seen in Table 3, the HF/6-31G(d) calculations were in good agreement with those of MP2/6-311++G(d,p), meaning that potential energy surface calculated by the HF level would reasonably represent that of MP2 level. Therefore, we carried out dynamics calculations of $CH_3(H_2O)_n$ complexes at the HF/6-31G(d) level.

3.2. Direct ab initio molecular dynamics calculations

3.2.1. Sample trajectory

In order to elucidate the finite temperature effects on the structures and HFCCs of the complexes, the direct ab initio MD calculations were performed at each temperature. The optimized structures were chosen as initial geometries at each simulation. The

Table 2
Calculated hyperfine coupling constants (HFCCs in G) of methyl radical, $CH_3(H_2O)$ and $CH_3(H_2O)_2$ complexes

	CH_3		$CH_3(H_2O)$		$CH_3(H_2O)_2$	
	H	C	H	C	H	C
MP2/6-311++G(d,p)//MP2/6-311++G(d,p)	−27.17	21.57	−26.28	22.13	−25.69	21.56
MP2/6-311++G(d,p)//HF/6-31G(d)	−27.16	20.96	−25.70	24.09	−25.38	23.02

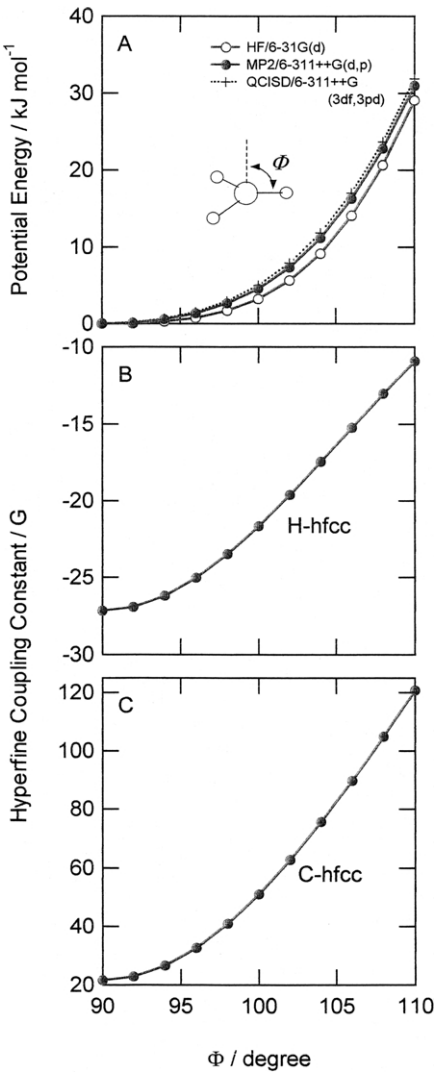

Fig. 2. Potential energy curves (A), hydrogen HFCC (B), and carbon HFCC (C), plotted as a function of bending angle (Φ) of CH_3. H- and C-HFCCs were calculated at the MP2/6-311++G(d,p) level.

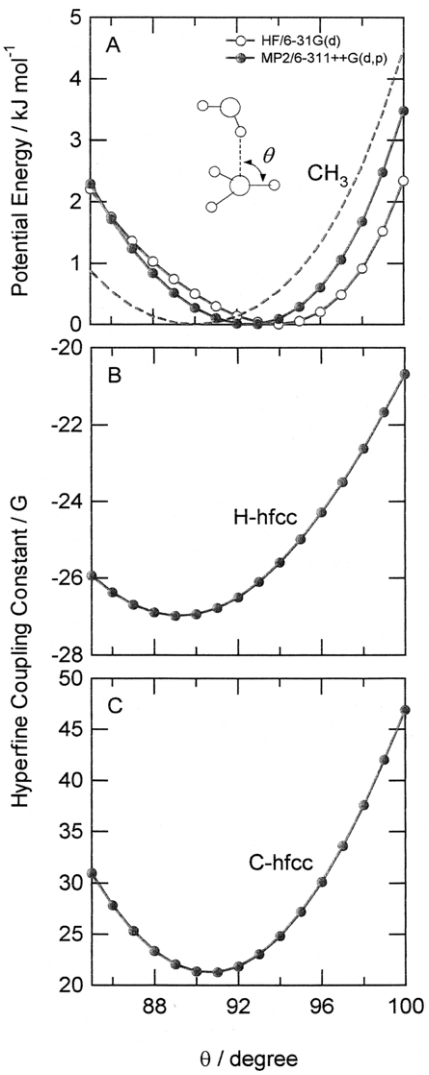

Fig. 3. The same as Fig. 2, but for the $CH_3(H_2O)$ complex. Dashed curve means potential energy curve for CH_3.

Table 3
Harmonic vibrational frequencies (cm^{-1}) of the $CH_3(H_2O)_n$ ($n = 0, 1, 2$) at the MP2/6-311++G(d,p) level and at the HF/6-31G(d) level in parenthesis; numbers in italic mean six modes of CH_3 in the complexes

Molecule	Frequencies (cm^{-1})			
CH_3	*3360 (3461)*	*3360 (3461)*	*3166 (3285)*	*1447 (1540)*
	1447 (1540)	*463 (308)*		
$CH_3(H_2O)$	3986 (4182)	3864 (4066)	*3358 (3456)*	*3356 (3454)*
	3164 (3280)	1633 (1831)	*1446 (1542)*	*1446 (1542)*
	547 (526)	223 (256)	186 (176)	93 (87)
	80 (78)	75 (75)	22 (12)	
$CH_3(H_2O)_2$	3970 (4169)	3969 (4157)	3841 (4055)	3781 (4016)
	3346 (3457)	*3344 (3443)*	*3150 (3273)*	1659 (1852)
	1640 (1829)	*1461 (1554)*	*1444 (1543)*	676 (685)
	617 (585)	450 (424)	268 (286)	249 (249)
	218 (205)	205 (179)	187 (175)	162 (146)
	116 (114)	102 (100)	90 (96)	75 (77)

result of the ab initio MD calculation for $CH_3(H_2O)$ is given in Fig. 4. The upper panel in Fig. 4 shows time dependence of intermolecular distance (R_{CO}), where R_{CO} is a distance between methyl-carbon of CH_3 and oxygen atoms of H_2O, and R_{CH} is one between the carbon atom of CH_3 and hydrogen atom in the first water. The intermolecular distance (R_{CO}) was widely varied from 3.56 to 3.72 Å at 10 K (the amplitude is 0.16 Å at 10 K), suggesting that the H_2O molecule is very weakly bound to the methyl radical. The amplitude of the intermolecular vibration increased with increasing temperature. At 50 K, the amplitude of R_{CO} was calculated to be 0.48 Å. Time dependence of R_{CH} was also analogous to that of R_{CO}. The large change of R_{CH} at 50 K originates from thermal activation of a direction of O–H bond of H_2O. This feature suggests that the position of H_2O molecule around the methyl radical is largely affected by the thermal activation.

The H- and C-HFCCs, which is proportional to contact spin density on nuclei, are plotted as a function of simulation time in Fig. 4 (middle and lower panels, respectively). The HFCCs for H and C atoms of CH_3 are only given. As clearly shown in Fig. 4, HFCCs for both H and C atoms are largely fluctuated as a function of simulation time. The amplitude becomes larger at higher temperatures, suggesting that the temperature affects strongly the HFCCs of CH_3 in the complexes, The change for the C atom was larger than that of the H atom. Therefore, it was concluded that the contact spin density is affected by thermal activation.

3.2.2. Temperature dependence of hyperfine coupling constants

As a summary of the trajectory calculations, HFCCs of CH_3 moiety calculated as a function of temperature were given in Fig. 5 (Table 4). The HFCCs are calculated at the MP2/6-311++G(d,p) level at each temperature. For methyl radical, H- and C-HFCCs were increased linearly with increasing temperature. On the other hand, H- and C-HFCCs of CH_3 moiety of $CH_3(H_2O)_n$ ($n = 1$ and 2) decreased as temperature is increased. It should be noted that the difference of H-HFCC of CH_3 moiety from those of free CH_3 was largest at 0 K.

4. Discussion

In the present study, we predicted temperature dependence of HFCCs of CH_3 of $CH_3(H_2O)_n$ ($n = 0–2$). The calculations showed that the HFCCs of CH_3 moiety in the complexes are strongly affected by thermal energy. For CH_3, H-HFCC increases with increasing temperature. In the case of $CH_3(H_2O)$ complex, H-HFCC at 0 K is calculated to be −26.28 G which is larger than that of CH_3 in vacuo (−27.17 G). This is due to the fact that structure of CH_3 is deformed by the interaction with H_2O: namely

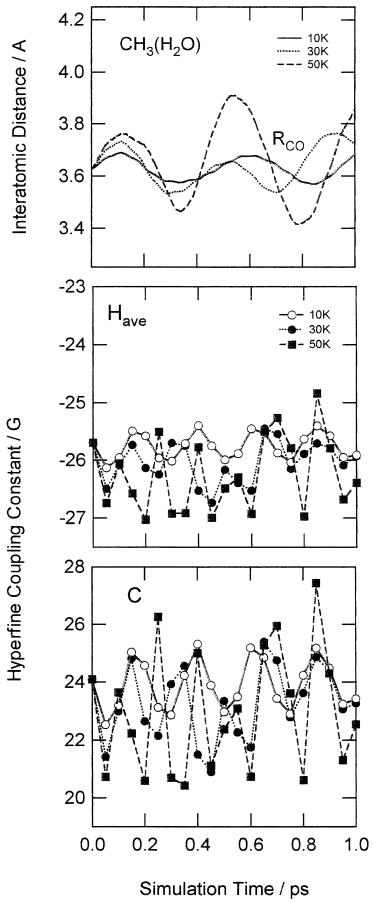

Fig. 4. Results of direct ab initio MD calculations for the $CH_3(H_2O)$ complex. (A) Time dependence of intermolecular distance (R_{CO}), (B) H-HFCCs of CH_3 moiety of $CH_3(H_2O)$, and (C) C-HFCCs. Temperatures were 10, 30, and 50 K. The ab initio MD calculations were carried out at the HF/6-31G(d) level, while H- and C-HFCCs were calculated at the MP2/6-311++G(d,p) level.

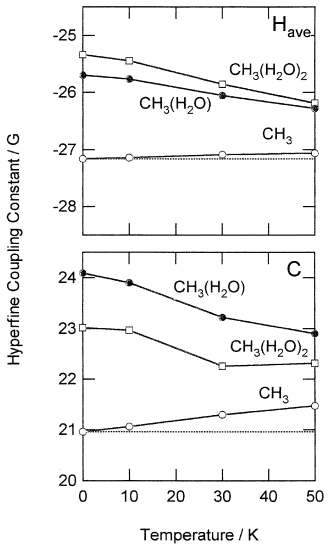

Fig. 5. Temperature dependence of the HFCCs of hydrogen and carbon of CH_3 in $CH_3(H_2O)_n$ ($n = 0$–2).

CH_3 has a bent form in $CH_3(H_2O)$ complex. H-HFCC of CH_3 in $CH_3(H_2O)$ also decreases with increasing temperature. The features in $CH_3(H_2O)_n$ ($n = 0$–2) are much different from that of CH_3 ($n = 0$). This can be explained as follows. The $CH_3(H_2O)$ complex has a weak binding energy (1.5 kcal/mol), so that H_2O can easily leave from CH_3 by thermal activation. Therefore, HFCC of CH_3 in $CH_3(H_2O)$ approaches gradually to that of CH_3 in vacuo at higher temperatures. For $CH_3(H_2O)_2$, H-HFCC of CH_3 was calculated to be -25.69 G. Temperature dependence of H-HFCC in $n = 2$ is very similar to that of $CH_3(H_2O)$ ($n = 1$).

Let us consider the solvation structure of CH_3 in bulk water and ice. The present calculations indicated that the binding energy of H_2O to CH_3 is only 1.5 kcal/mol, which is less than that of water–water hydrogen bond (≈ 5–8 kcal/mol). H_2O will prefer to

Table 4
Hyperfine coupling constants of hydrogen- and carbon atoms of the CH_3 in $CH_3(H_2O)_n$ complexes (in Gauss) calculated by direct ab initio MD calculations

T (K)	H($n = 0$)	H($n = 1$)	H($n = 2$)	C($n = 0$)	C($n = 1$)	C($n = 2$)
0	−27.16	−25.70	−25.34	20.96	24.09	23.02
10	−27.14	−25.77	−25.45	21.06	23.90	22.97
30	−27.09	−26.06	−25.86	21.29	23.22	22.25
50	−27.06	−26.28	−26.19	21.47	22.90	22.31

bind to a neighboring water molecule rather than CH_3. Therefore, the methyl radical exists as isolated radical in bulk or in ice. The hyperfine structure of CH_3 is thus observed as an isotropic value in matrices. The complex $CH_3(H_2O)_n$ ($n = 1, 2$) would be observed in gas phase or in rare gas matrix. This feature is consistent with previous experiments [25–27].

The vibrational effects on the HFCC of CH_3 have been investigated theoretically by several groups [28,29] Cramer calculated HFCC of CH_3 by solving one-dimensional vibrations Schrodinger equation. The HFCC of hydrogen of CH_3 (H-HFCC) for vibrational levels $n = 0$, 1 and 2 were -25.6, -22.6 and -20.6 G, respectively. Boltzmann averaged at 77 K was calculated to be -25.6 G. This result indicates that H-HFCC of CH_3 increases with increasing temperature. Barone et al. also obtained the similar results. The present calculations are essentially agreed with the results obtained by one-dimensional quantum mechanical calculations. However, the increase of H-HFCC obtained from our full dimensional trajectory calculations was slightly larger than that of one-dimensional calculations. This implies that both C-H symmetric and asymmetric vibrations affects slightly H-HFCC as well as umbrella mode.

In the present study, we have introduced several approximations to calculate the potential energy and to treat the reaction dynamics. Firstly, we assumed that the atom behaves as a classical particle in the multi-dimensional potential energy surface. The quantum effect was not considered in the present calculations. This may cause slight change of the HFCC at very low temperature and the dynamics of the complex. Secondly, we assumed HF/6-31G(d) multi-dimensional potential energy surface in the trajectory calculations throughout. By using the geometry generated by HF/6-31G(d) dynamics calculation, HFCCs are calculated at the MP2/6-311++G(d,p) level. The dynamics calculation with more accurate wave function may provide deeper insight in the detailed dynamics.

In the trajectory calculations, zero-point vibrational energy (ZPE) was neglected. This approximation means that the dynamics effect on H-HFCC is zero at 0 K. At high temperature, the difference between the classical and quantum averages becomes smaller. Therefore, it should be noted that this model is limited at higher temperature above ca. 10 K. Despite the several assumptions introduced here, the results enable us to obtain valuable information on the finite temperature effect on the spin density on the weakly bonded complex.

Acknowledgments

The authors are indebted to the Computer Center at the Institute for Molecular Science (IMS) for the use of the computing facilities. The authors acknowledge partial support from a Grant-in-Aid from the Ministry of Education, Science, Sports and Culture of Japan.

References

[1] A. Romieu, S. Bellon, D. Gaparutto, J. Cadet, Org. Lett. 2 (2000) 1085.
[2] S. Hix, M.B. Kadiis, R.P. Mason, O. Augusto, Chem. Res. Toxicol. 13 (2000) 1056.
[3] A. Lund, M. Shiotani, in: A. Lund (Ed.), Radical Ionic Systems, Kluwer, Dordrecht, 1991.
[4] R. Zhu, C.C. Hsu, M.C. Lin, J. Chem. Phys. 115 (2001) 195.
[5] R.A. Eng, A. Gebert, E. Goos, H. Hippler, C. Kachiani, Phys. Chem. Chem. Phys. 3 (2001) 2258.
[6] C. Yamada, E. Hirota, K. Kawaguchi, J. Chem. Phys. 75 (1981) 5256.
[7] D.M. Chipman, J. Chem. Phys. 78 (1983) 3112.
[8] S. Lunell, L.A. Eriksson, T. Fangstrom, J. Maruani, L. Sjoqvist, A. Lund, Chem. Phys. 171 (1993) 119.
[9] M.-B. Huang, S. Lunell, K. Karlsson, Chem. Phys. Lett. 171 (1990) 265.
[10] Y. Itagaki, M. Shiotani, H. Tachikawa, Acta. Chim. Scand. 51 (1997) 220.
[11] E.Y. Misochko, V.A. Benderskii, A.U. Goldschleger, A.V. Akimov, A.F. Schestakov, J. Am. Chem. Soc. 117 (1995) 11997.
[12] H. Tachikawa, J. Phys. Chem. A 102 (1998) 7065.
[13] H. Tachikawa, M. Igarashi, T. Ishibashi, Chem. Phys. Lett. 352 (2002) 113.
[14] K.V. Rao, M.C.R. Symons, J. Chem. Soc. A (1971) 2163.
[15] L. Andrews, M. Moskovist (Eds.), Chemistry and Physics of Matrix-Isolated Species, Elsevier, Amsterdam, 1989, and references therein.
[16] B.S. Jursic, Chem. Phys. Lett. 244 (1995) 263.
[17] Y. Chen, E. Tshkuikow-Roux, A. Rauk, J. Phys. Chem. 95 (1991) 9832.
[18] M.J. Frisch, G.W. Trucks, H.B. Schlegel, G.E. Scuseria, M.A. Robb, J.R. Cheeseman, V.G. Zakrzewski, J.A. Montgomery, Jr., R.E. Stratmann, J.C. Burant, S. Dapprich, J.M. Millam, A.D. Daniels, K.N. Kudin, M.C. Strain, O. Farkas, J. Tomasi, V. Barone, M. Cossi, R. Cammi, B. Mennucci, C. Pomelli, C. Adamo, S. Clifford, J. Ochterski, G.A. Petersson,

P.Y. Ayala, Q. Cui, K. Morokuma, D.K. Malick, A.D. Rabuck, K. Raghavachari, J.B. Foresman, J. Cioslowski, J.V. Ortiz, B.B. Stefanov, G. Liu, A. Liashenko, P. Piskorz, I. Komaromi, R. Gomperts, R.L. Martin, D.J. Fox, T. Keith, M.A. Al-Laham, C.Y. Peng, A. Nanayakkara, C. Gonzalez, M. Challacombe, P.M.W. Gill, B. Johnson, W. Chen, M.W. Wong, J.L. Andres, C. Gonzalez, M. Head-Gordon, E.S. Replogle, J.A. Pople, Ab initio MO program GAUSSIAN 98, Revision A.5, Gaussian, Pittsburgh, PA, 1998.

[19] H. Tachikawa, M. Igarashi, J. Phys. Chem. A 102 (1998) 8648.

[20] H. Tachikawa, M. Igarashi, Chem. Phys. Lett. 303 (1999) 81.

[21] H. Tachikawa, J. Phys. Chem. A 104 (2000) 7788.

[22] H. Tachikawa, J. Phys. Chem. A 105 (2001) 1260.

[23] H. Tachikawa, J. Phys. Chem. A 103 (1999) 2501.

[24] H. Tachikawa, J. Phys. B 33 (2000) 1725.

[25] A. Campion, F. Williams, J. Am. Chem. Soc. 94 (1972) 7633.

[26] R.L. Hudson, M. Shiotani, F. Williams, Chem. Phys. Lett. 48 (1977) 193.

[27] T. Doba, K.U. Ingold, W. Siebrand, Chem. Phys. Lett. 103 (1984) 339.

[28] C.J. Ceamer, J. Org. Chem. 56 (1991) 5229.

[29] V. Barone, A. Grad, C. Minichino, R. Subra, J. Chem. Phys. 99 (1993) 6787.